

Stepwise Construction of the Cr–Cr Quintuple Bond and Its Destruction upon Axial Coordination**

Yu-Lun Huang, Duan-Yen Lu, Hsien-Cheng Yu, Jen-Shiang K. Yu, Chia-Wei Hsu, Ting-Shen Kuo, Gene-Hsiang Lee, Yu Wang, and Yi-Chou Tsai*

Although quadruple bonding in transition-metal chemistry has been considered a thoroughly studied area,^[1a] the concept of multiple bonding^[1b] was reinvigorated in 2005 by the seminal discovery of the first Cr–Cr quintuple bond in the isolable dimeric chromium compound Ar'CrCrAr' (Ar' = 2,6-(2,6-*i*Pr₂C₆H₃-)₂C₆H₃) by Power and co-workers.^[2] Since then, the structures of several Group 6 homobimetallic compounds with very short Cr–Cr (1.73–1.75 Å) and Mo–Mo (2.02 Å) quintuple bonds have been characterized.^[3] All these remarkable quintuple-bonded bimetal units are supported by either C- or N-based bridging ligands. Based on their structures, these quintuple-bonded dinuclear compounds can be simply classified into two types as illustrated in Figure 1. The

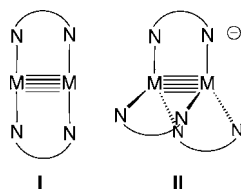


Figure 1. Two types of quintuple-bonded complexes.

existence of the type I quintuple bond was recently corroborated by experiments,^[4a] and the bonding paradigms of both types were realized by theoretical investigations.^[4] Preliminary reactivity studies on the type I complexes show that they are reactive towards the activation of small molecules and display interesting complexation with olefins and alkynes.^[5]

Up to now, both type I and II compounds have been exclusively synthesized by a procedure analogous to the

Wurtz reductive coupling reaction of the corresponding chloride coordinated precursors.^[2,3] The previously reported quintuple-bonded dichromium examples were obtained by alkali metal reduction of the mononuclear [LCrCl₂(THF)₂]^[3c,e] or dimeric complexes [LCr(μ-Cl)]₂^[3] (L = monodentate or bidentate ligand). It should be noted that all these precursors lack Cr–Cr bonding. Besides, we have recently demonstrated that the metal–metal quintuple and quadruple bond can be constructed from the corresponding quadruple and triple bond, respectively. For example, the δ bonds in the quintuple-bonded species [Mo₂{μ-η²-RC(N-2,6-*i*Pr₂C₆H₃)₂}]₂ (R = H, Ph)^[3h] and quadruple-bonded complex [Mo₂{μ-η²-Me₂Si(N-2,6-*i*Pr₂C₆H₃)₂}]₂^[6] are formed by alkali metal reduction of the corresponding chloride-coordinated quadruple- and triple-bonded species, respectively. However, the formation mechanism of the metal–metal quintuple bonds has not been investigated. To this end, continuing our exploration in the field of quintuple-bond chemistry, we herein report the construction of a complex with a Cr–Cr quintuple bond by two subsequent one-electron-reduction steps from a halide-free homo-divalent dichromium complex to a mixed-valent intermediate (Cr^I, Cr^{II}), and then to the final quintuple-bonded product. Structural characterization of these dichromium compounds is important to shed light on the formation mechanism of the metal–metal quintuple bonds. Moreover, the metal–metal quadruple bonds can be dramatically elongated by intramolecular axial coordination, but such an interaction in the quintuple-bonding system has not been investigated. We report herein that the Cr–Cr quintuple bond can be readily cleaved by disproportionation induced by intramolecular axial coordination.

As illustrated in Scheme 1, treatment of CrCl₂ in THF with 1 equiv of dilithiated 2,6-diamidopyridine Li₂[2,6-(2,6-*i*Pr₂C₆H₃-N)₂-4-CH₃C₅H₂N] (**1**) and Li₂[2,6-(*i*Pr₃SiN)₂-C₅H₃N] (**2**), prepared by adding 2 equiv of *n*BuLi to the corresponding 2,6-diaminopyridine in *n*-hexane, yields two dark green dimeric complexes [(THF)Cr(μ-κ¹:κ²-2,6-(2,6-*i*Pr₂C₆H₃-N)₂-4-CH₃C₅H₂N)]₂ (**3**) and [(THF)Cr(μ-κ¹:κ²-2,6-(*i*Pr₃SiN)₂-C₅H₃N)]₂ (**4**), respectively, in good yields (62% for **3** and 74% for **4**). The ¹H NMR spectra of **3** and **4** display broad signals in the range of 20 and –10 ppm, so little useful information could be obtained.

The dinuclear nature of **3** and **4** was confirmed by single-crystal X-ray crystallography^[7] and their molecular structures are depicted in Figure 2 and Figure S2 in the Supporting Information). It is interesting to note that although these two dinuclear species bear the same number of ligands, they exhibit very different structural conformations. In compound **3**, each Cr atom is five-coordinate, ligated by four nitrogen

[*] Y.-L. Huang, D.-Y. Lu, H.-C. Yu, C.-W. Hsu, Prof. Dr. Y.-C. Tsai
Department of Chemistry and Frontier Research Center on
Fundamental and Applied Sciences of Matters
National Tsing Hua University, Hsinchu 30013 (Taiwan)
E-mail: yictai@mx.nthu.edu.tw

Prof. Dr. J.-S. K. Yu
Institute of Bioinformatics and Systems Biology and
Department of Biological Science and Technology
National Chiao Tung University, Hsinchu, 30010 (Taiwan)
T.-S. Kuo

Department of Chemistry
National Taiwan Normal University, Taipei 11677 (Taiwan)

Dr. G.-H. Lee, Prof. Dr. Y. Wang
Department of Chemistry
National Taiwan University, Taipei 10617 (Taiwan)

[**] We are grateful to the National Science Council, Taiwan for financial support under grants NSC 99-2113M-007-012-MY3 (Y.C.T.) and 100-2627-B-009-001 (J.S.K.Y.), and the “Center for Bioinformatics Research of Aiming for the Top University Program” of NCTU and MoE, Taiwan.

Supporting information for this article (including experimental details for the synthesis and characterization of complexes **3**–**8**) is available on the WWW under <http://dx.doi.org/10.1002/ange.201202337>.

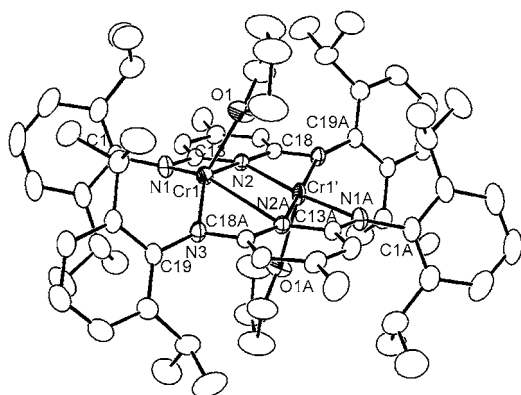
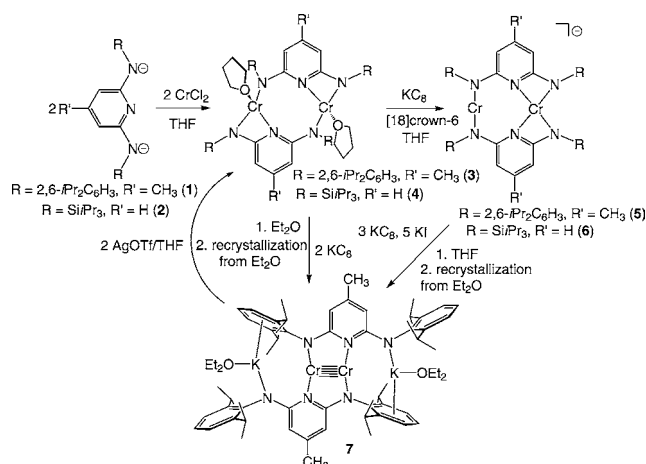


Figure 2. Molecular structure of **3** with thermal ellipsoids at 35% probability. Hydrogen atoms have been omitted for clarity.

donors and a molecule of THF, but the Cr atoms in **4** are four-coordinate, surrounded by three nitrogen atoms and a THF molecule. In **3**, the two 2,6-diamidopyridyl ligands are parallel to each other and two THF ligands are arranged in an *anti* conformation. The two much more sterically encumbered silyl-substituted 2,6-diamidopyridyl ligands in **4**, however, are arranged in a nearly orthogonal orientation with a torsion angle of 77.5(1)° with two THF ligands in a *syn* conformation. Each Cr atom in **3** adopts a square-pyramidal geometry, but the geometry at each Cr atom in **4** is approximately planar. As a result, compound **3** has a shorter Cr–Cr distance of 2.8513(25) Å, while the separation between two chromium centers is 3.1151(7) Å in **4**. Despite the significant structural differences, **3** and **4** display similar magnetic properties. The room-temperature solution magnetic moments of **3** and **4** are 4.22 and 3.89 μ_B , respectively, which are both less than the spin-only value expected for two uncoupled Cr^{2+} ions ($\mu_{\text{eff}} = 6.93$ for $S_1 = S_2 = 2$), indicative of antiferromagnetic coupling.

Subsequent one-electron reduction of dark green **3** and **4** in THF by 1 equiv of KC_8 in the presence of 1 equiv of [18]crown-6 and recrystallization from diethyl ether and THF gives the reddish brown mixed-valent dinuclear complex

$[(\text{Et}_2\text{O})\text{K}][18\text{crown-6}][\text{Cr}\{\mu\text{-}\kappa^1\text{:}\kappa^2\text{-}2,6\text{-(}2,6\text{-}i\text{Pr}_2\text{C}_6\text{H}_3\text{-N)}_2\text{-}4\text{-CH}_3\text{C}_5\text{H}_2\text{N)}_2\text{Cr}]$ (**5**) (43% yield) and brown $[(\text{THF})_2\text{K}][18\text{crown-6}][\text{Cr}\{\mu\text{-}\kappa^1\text{:}\kappa^2\text{-}2,6\text{-(}i\text{Pr}_3\text{Si-N)}_2\text{C}_5\text{H}_3\text{N)}_2]$ (**6**) (35% yield), respectively. Like **3** and **4**, the ^1H NMR spectra of **5** and **6** are also not diagnostic because of the extreme line broadening caused by their nondiamagnetic properties.

Fortunately, the formulation of **5** and **6** was corroborated by X-ray crystallography,^[7] and their molecular structures are depicted in Figure 3 ($[(\text{Et}_2\text{O})\text{K}[18\text{-crown-6}][\text{5}])$ and Fig-

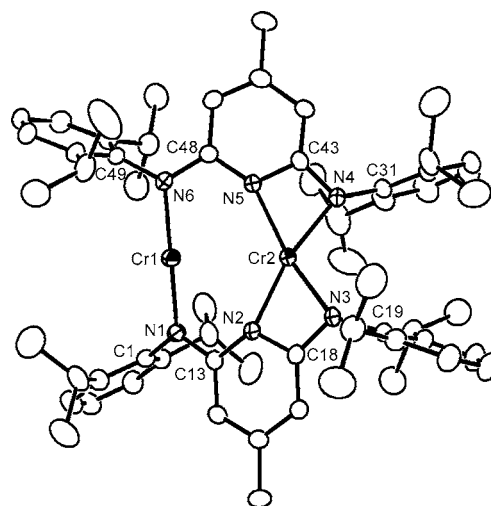


Figure 3. Molecular structure of the Cr-containing anion of **5** with thermal ellipsoids at 35% probability. The counter cation $[(\text{Et}_2\text{O})\text{K}[18\text{crown-6}]^+$, diethyl ether solvate, and hydrogen atoms have been omitted for clarity.

ure S4 ($[(\text{THF})_2\text{K}[18\text{-crown-6}][\text{6}])$). Unlike **3** and **4** and their striking structural difference, compounds **5** and **6** display strongly similar structures. In contrast to **3**, the two 2,6-diamidopyridyl units in **5** are no longer parallel; the dihedral angle between these two supporting ligands is 33.4(2)°. In **6**, the torsion angle between two pyridyl units is 52.7(3)°. Both compounds consistently show two chromium atoms in different coordination environments. One chromium atom is ligated by two N donors (amido) and thus shows a linear geometry with the bond angle N1-Cr1-N6 of 178.00(17)° in **5** and N3-Cr2-N3A of 177.8(2)° in **6**, while the other chromium atom is embraced by the other four nitrogen atoms and thus displays a roughly planar conformation. In comparison with two structurally characterized monomeric two-coordinate monovalent chromium complexes $[(2,6\text{-(}2,4,6\text{-}i\text{Pr}_3\text{C}_6\text{H}_2)_2\text{-}3,5\text{-}i\text{Pr}_2\text{C}_6\text{H}_3)\text{Cr}(\text{L})]$ ($\text{L} = \text{THF}, \text{PMe}_3$), in which the central Cr atom has five unpaired electrons described by Power and co-workers,^[8] a +1 oxidation state is accordingly assigned to the two-coordinate chromium centers, while the four-coordinate chromium centers are divalent. The distances between two Cr atoms are 3.1036(11) (**5**) and 2.9277(15) Å (**6**), indicative of no Cr–Cr bond. Besides the structural resemblance, **5** and **6** also possess similar magnetic properties. They both exhibit an antiferromagnetic exchange between two Cr spin centers. The room-temperature solution magnetic moments of **5** and **6** are 5.00 and 3.53 μ_B , respectively, which are less than the spin-only

value expected for two noninteracting Cr^+ and Cr^{2+} ions ($\mu_{\text{eff}} = 7.68$ for $S_1 = 5/2$ and $S_2 = 2$).

Interestingly, when a solution of **3** in diethyl ether is treated with 2.5 equiv of KC_8 , the diamagnetic burgundy Cr–Cr quintuple-bonded complex $[(\text{Et}_2\text{O})\text{K}]_2\{\text{Cr}_2(\mu\text{-}\kappa^1\text{:}\kappa^1\text{:}\eta^3\text{:}\eta^6\text{-}2,6\text{-}(2,6\text{-iPr}_2\text{C}_6\text{H}_3\text{-N})_2\text{-}4\text{-CH}_3\text{C}_5\text{H}_2\text{N})_2\}$ (**7**) is isolated (43 % yield) after recrystallization from diethyl ether. In contrast, treatment of **4** with an excess amount (4 equiv) of KC_8 does not engender the formation of the analogous Cr–Cr quintuple-bonded species. Complex **7** can be prepared alternatively by reduction of **5** in THF with KC_8 (3 equiv), but the yield of isolated product is poor (6%). It is, however, interesting to note that the yield of **7** can be dramatically improved to 82 %, if 5 equiv of potassium iodide is added. Interestingly, the reaction of **6** and 3 equiv of KC_8 in the presence of 5 equiv of potassium iodide does not give the Cr–Cr quintuple-bonded species, either.

The formulation of **7** is supported by the ^1H NMR spectrum. For example, signals corresponding to only one ligand environment are observed at room temperature. Two different *meta* protons of the pyridine backbone resonate at $\delta = 4.89$ and 4.61 ppm with an integration ratio of 1:1. The ratio of the K^+ ion bound diethyl ether to 2,6-diamidopyridyl ligand is 1:1 as well. The solid-state molecular structure of **7** was established by X-ray crystallography^[7] and is presented in Figure 4. Complex **7** displays C_{2h} symmetry with the Cr_2 unit lying on the crystallographically imposed center of symmetry.

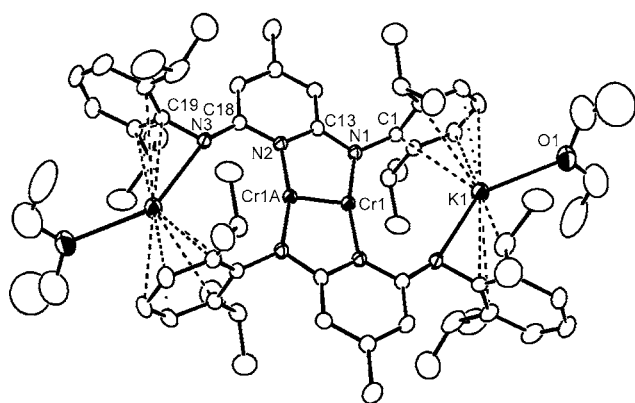


Figure 4. Molecular structure of **7** with thermal ellipsoids at 35 % probability. The diethyl ether solvate and hydrogen atoms have been omitted for clarity.

In principle, the core structure of **7** belongs to the type I conformation. Each ligand uses two of its three nitrogen atoms to coordinate with the Cr_2 unit. The third nitrogen, located near one of the two chromium atoms in an off-axis position, is blocked by coordinating with a K^+ ion. Thus, the directions of the two pendant arms alternate around the dichromium unit. One striking feature is the extremely short Cr–Cr bond length of 1.7443(10) Å, comparable to those of the type I 2-amidopyridine- and amidinate-stabilized quintuple-bonded dichromium complexes.^[3c,e] The Cr–Cr quintuple bond is sensitive to oxidation. Two-electron oxidation of **7** upon treatment with 2 equiv of AgOTf in THF results in the

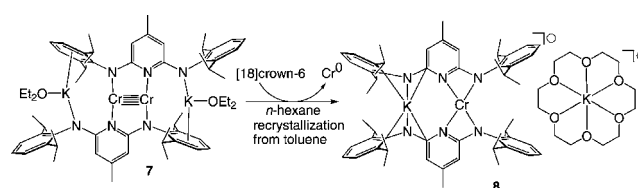
cleavage of the Cr–Cr quintuple bond and gives **3** in quantitative yield.

The magnetic susceptibility of **7** was measured between 2 and 300 K. Simulation based on a best fit of the data points yielded a temperature-independent paramagnetism (TIP) = 768×10^{-6} emu (Figure S6), which is consistent with Power's quintuple-bonded dichromium compounds with TIP values of 680×10^{-6} to 1500×10^{-6} emu.^[2,3a] This magnetic behavior indicates an $S = 0$ ground state, which supports strongly coupled $d^5\text{--}d^5$ bonding electrons.

On the theoretical side, the DFT calculations at the BP86 level with triple- ζ quality basis sets gave a theoretical structure for **7** in good agreement with the X-ray data (see Table S13 in the Supporting Information). As indicated by the molecular orbital (MO) studies, there is no significant N–Cr π -bonding interactions. Attention is next drawn to five occupied metal-based MOs, namely, HOMO, HOMO-1, HOMO-4, HOMO-6, and HOMO-10 (see Figure S7 in the Supporting Information). These orbitals have their electron densities concentrated on the metal atoms rather than the supporting ligands and thus may be assumed to be responsible for the metal–metal bonding. Among these five occupied Cr–Cr bonding MOs, HOMO-10 ($d_{yz}\text{--}d_{yz}$) and HOMO-6 ($d_{xz}\text{--}d_{xz}$) represent two Cr–Cr π bonds, while the Cr–Cr σ character is found at HOMO-4 ($(d_{z^2} + d_{z^2})$). The contour plots of HOMO ($d_{xy} + d_{xy}$) and HOMO-1 ($(sd_{x^2-y^2} + sd_{x^2-y^2})$) unambiguously indicate two Cr–Cr δ bonds. Overall, the pattern of these five occupied metal–metal bonding MOs leads to an effective bond order (eBO) of 4.54.^[9] The Cr–Cr bond in **7** is formally quintuple, because five orbitals and five electrons on each Cr atom are involved in the bonding.

Another striking structural feature of **7** is the presence of two potassium counter cations, which are ligated by amido nitrogen atoms and capped by neighboring phenyl rings. In fact, the encapsulated K^+ ions in **7** play a critical role in the formation of the Cr–Cr quintuple bond. In contrast to ligand **1**, the lack of two N(amido)-substituted aryl groups, which can stabilize the K^+ ions, renders ligand **2** unable to support the quintuple-bonded Cr_2 unit. Presumably, over the course of the reduction of **5**, the coordination of the lone pairs of the pendant amido nitrogen atoms to K^+ ions, by which the interaction between Cr atoms and pendant nitrogen atoms can be blocked, makes further one-electron reduction of **5** and formation of **7** possible. The presence of two K^+ ions in **7** is thus of vital importance towards the stabilization the quintuple-bonded Cr_2 unit. This speculation is corroborated by the following experiment.

Compound **7** is stable in *n*-hexane and diethyl ether. However, addition of 1 equiv of [18]crown-6 ether to a burgundy suspension of **7** in *n*-hexane unexpectedly elicited



Scheme 2. The reaction of **7** and 1 equiv of [18]crown-6.

formation of a dark brown precipitate (Scheme 2). After recrystallization from toluene, the brown mononuclear tetra-coordinate divalent chromium complex $[(\eta^3\text{-CH}_3\text{C}_6\text{H}_5)\text{K}-\text{C}[18\text{-crown-6}][\text{K}\{\mu\text{-}\eta^1\text{:}\kappa^1\text{:}\eta^1\text{:}\kappa^2\text{-2,6-(2,6-}i\text{Pr}_2\text{C}_6\text{H}_3\text{-N)}_2\text{-4-CH}_3\text{-C}_5\text{H}_2\text{N)}_2\text{Cr}]\text{ (8)}$ was isolated in very good yield (89%). The molecular structure of **8** was established by X-ray crystallography (see Figure S8 in the Supporting Information). It is not clear as to how compound **7** undergoes Cr_2^{2+} disproportionation to produce **8**. Two possible pathways are proposed for this reaction. One is that the crown ether first coordinates one of the chromium atoms, which consequently becomes more electron-rich, and is able to reduce the other chromium atom. The other possibility is that upon removal of one K^+ ion by the crown ether, the lone pair of the pendant amido nitrogen atom binds the nearby chromium atom, which renders the three-coordinate chromium atom more electron-rich, and then reduces the two-coordinate chromium atom to give **8**. Such axial coordination is possible because the distance between chromium and the potassium-bound nitrogen atom is 3.079(3) Å, which is comparable to the distances (2.734(3)–3.089(6) Å) between Cr and the pendant nitrogen atoms in the quadruple-bonded dichromium complexes $[\text{Cr}_2(\text{DPhIP})_4]$ and $[\text{Cr}_2(\text{dpa})_4]$ (DPhIP = 2,6-di(phenylimino)piperidinate, dpa = 2,2'-dipyridylamide).^[10] These short Cr...N contacts in the latter two compounds result in remarkable elongation of the Cr–Cr quadruple bonds. For instance, the Cr–Cr distance is 2.2652(9) Å in $[\text{Cr}_2(\text{DPhIP})_4]\cdot\text{THF}$, while it is 1.858(1) Å in $[\text{Cr}_2(\text{PhIP})_4]$ (PhIP = phenyliminopiperidinate) without pendant nitrogen atoms.^[10]

In the chemistry of complexes with quadruple metal–metal bonds, axial coordination usually results in significant elongation of the metal–metal bond lengths.^[1a] For example, the Cr–Cr distances range from 2.688(1) Å^[11] (no Cr–Cr bonding) in complexes having strong axial coordination to 1.773(1) Å^[12] in those without it. This is also the case in the chemistry of complexes with quintuple metal–metal bonds. Recrystallization of the quintuple-bonded dimeric chromium amidinate $[(\text{Cr}(\mu\text{-}\kappa^1\text{:}\kappa^1\text{-HC(N-2,6-Me}_2\text{C}_6\text{H}_3)_2)]_2$ (**9**), where the Cr–Cr bond length is 1.7404(8) Å,^[3c] from weakly coordinating THF and 2-methylfuran (2-MeTHF) afforded the axially ligated complexes $[(\text{THF})\text{Cr}(\mu\text{-}\kappa^1\text{:}\kappa^1\text{-HC(N-2,6-Me}_2\text{C}_6\text{H}_3)_2)]_2$ (**10**) and $\{(2\text{-MeTHFCr})\text{Cr}[(\mu\text{-}\kappa^1\text{:}\kappa^1\text{-HC(N-2,6-Me}_2\text{C}_6\text{H}_3)_2)]_2\}$ (**11**), respectively. The molecular structures of **10** and **11** were determined by X-ray crystallography^[7] and are depicted in Figures S9 and S10, respectively. It is interesting to note that the ligated THF and 2-MeTHF in **10** and **11** are very labile. As assayed by ¹H NMR spectroscopy, upon dissolution of **10** and **11** in C_6D_6 , the THF and 2-MeTHF ligands completely dissociate from the Cr_2 unit. The high lability of both poor σ -donors is also supported by the long Cr...O distances, 2.579(4) Å (**10**) and 2.305(7) Å (**11**). Interestingly, the strength of the Cr–Cr quintuple bond is indeed weakened by axial coordination. As indicated by the structural parameters, the separation between two Cr centers in **10** and **11** is 1.8115(12) and 1.7634(5) Å, respectively, which are significantly longer than that of **9**.

In conclusion, the new type I Cr–Cr quintuple-bonded compound **7** supported by two terdentate 2,6-diamidopyridyl ligands has been prepared by a sequential reduction proce-

ducing starting from a halide-free precursor. The employment of the terdentate 2,6-diamidopyridyl ligands has not only allowed for the isolation and X-ray structural characterization of the quintuple-bonded Cr_2 compound **7**, but also the mixed-valent (Cr^{I} and Cr^{II}) intermediates **5** and **6**. The characterization of **5** and **6** is of importance to elucidate the formation mechanism of the type I quintuple-bonded complexes. Besides, the 2,6-diamidopyridine ligand provides a platform to investigate how an axial interaction affects the length of the Cr–Cr quintuple bond. In contrast to the elongation of the Cr–Cr quadruple bonds caused by axial coordination, the Cr–Cr quintuple bond of **7** can be ruptured by disproportionation induced by axial ligation. Reactivity studies on **5**, **6**, and **7** are currently underway.

Received: March 24, 2012

Revised: May 9, 2012

Published online: June 22, 2012

Keywords: amidinate · axial coordination · chromium · formation mechanism · quintuple bonds

- [1] a) F. A. Cotton, C. A. Murillo, R. A. Walton, *Multiple Bond Between Metal Atoms*, Springer, Berlin, 3rd ed., **2005**; b) F. R. Wagner, A. Noor, R. Kempe, *Nat. Chem.* **2009**, *1*, 529.
- [2] T. Nguyen, A. D. Sutton, S. Brynda, J. C. Fetting, G. J. Long, P. P. Power, *Science* **2005**, *310*, 844.
- [3] a) R. Wolf, C. Ni, T. Nguyen, M. Brynda, G. J. Long, A. D. Sutton, R. C. Fischer, J. C. Fetting, M. Hellman, L. Pu, P. P. Power, *Inorg. Chem.* **2007**, *46*, 11277; b) K. A. Kreisel, G. P. A. Yap, P. O. Dmitrenko, C. R. Landis, K. H. Theopold, *J. Am. Chem. Soc.* **2007**, *129*, 14162; c) A. Noor, F. R. Wagner, R. Kempe, *Angew. Chem.* **2008**, *120*, 7356; *Angew. Chem. Int. Ed.* **2008**, *47*, 7246; d) Y.-C. Tsai, C.-W. Hsu, J.-S. K. Yu, G.-H. Lee, Y. Wang, T.-S. Kuo, *Angew. Chem.* **2008**, *120*, 7360; *Angew. Chem. Int. Ed.* **2008**, *47*, 7250; e) C.-W. Hsu, J.-S. K. Yu, C.-H. Yen, G.-H. Lee, Y. Wang, Y.-C. Tsai, *Angew. Chem.* **2008**, *120*, 10081; *Angew. Chem. Int. Ed.* **2008**, *47*, 9933; f) A. Noor, G. Glatz, R. Müller, M. Kaupp, S. Demeshko, R. Kempe, *Z. Anorg. Allg. Chem.* **2009**, *635*, 1149; g) Y.-C. Tsai, H.-Z. Chen, C.-C. Chang, J.-S. K. Yu, G.-H. Lee, Y. Wang, T.-S. Kuo, *J. Am. Chem. Soc.* **2009**, *131*, 12534; h) S.-C. Liu, W.-L. Ke, J.-S. K. Yu, T.-S. Kuo, Y.-C. Tsai, *Angew. Chem.* **2012**, DOI: 10.1002/ange.201200122; *Angew. Chem. Int. Ed.* **2012**, DOI: 10.1002/anie.201200122.
- [4] a) L.-C. Wu, C.-W. Hsu, Y.-C. Chuang, G.-H. Lee, Y.-C. Tsai, Y. Wang, *J. Phys. Chem. A* **2011**, *115*, 12602; b) L. Gagliardi, B. O. Roos, *Lect. Ser. Comput. Comput. Sci.* **2006**, *6*, 6; c) M. Brynda, L. Gagliardi, P.-O. Widmark, P. P. Power, B. O. Roos, *Angew. Chem.* **2006**, *118*, 3888; *Angew. Chem. Int. Ed.* **2006**, *45*, 3804; d) B. O. Roos, A. C. Borin, L. Gagliardi, *Angew. Chem.* **2007**, *119*, 1491; *Angew. Chem. Int. Ed.* **2007**, *46*, 1469; e) G. La Macchia, L. Gagliardi, P. P. Power, M. Brynda, *J. Am. Chem. Soc.* **2008**, *130*, 5104; f) G. La Macchia, F. Aquilante, V. Veryazov, B. O. Roos, L. Gagliardi, *Inorg. Chem.* **2008**, *47*, 11455; g) M. Brynda, L. Gagliardi, B. O. Roos, *Chem. Phys. Lett.* **2009**, *471*, 1; h) G. La Macchia, G. Li Manni, T. K. Todorova, M. Brynda, F. Aquilante, B. O. Roos, L. Gagliardi, *Inorg. Chem.* **2010**, *49*, 5216.
- [5] a) A. Noor, G. Glatz, R. Müller, M. Kaupp, S. Demeshko, R. Kempe, *Nat. Chem.* **2009**, *1*, 322; b) C. Ni, B. D. Ellis, G. J. Long, P. P. Power, *Chem. Commun.* **2009**, 2332; c) A. Noor, E. S. Tamne, S. Qayyum, T. Bauer, R. Kempe, *Chem. Eur. J.* **2011**, *17*, 6900; d) C. Schwarzmaier, A. Noor, G. Glatz, M. Zabel, A. Y.

- Timoshkin, B. M. Cossairt, C. C. Cummins, R. Kempe, M. Scheer, *Angew. Chem.* **2011**, 123, 7421; *Angew. Chem. Int. Ed.* **2011**, 50, 7283; e) J. Shen, G. P. A. Yap, J.-P. Werner, K. H. Theopold, *Chem. Commun.* **2011**, 47, 12191.
- [6] Y.-C. Tsai, Y.-M. Lin, J.-S. K. Yu, J.-K. Hwang, *J. Am. Chem. Soc.* **2006**, 128, 13980.
- [7] Crystallographic data for **3**-*n*-C₆H₁₄: C₇₄H₁₀₈N₆Cr₂O₂, *M_r* = 1217.66, *T* = 200(2) K, triclinic, space group *P* $\bar{1}$, *a* = 10.9399(15), *b* = 13.3874(19), *c* = 14.825(2) Å, *α* = 70.668(2), *β* = 70.474(2), *γ* = 79.147(2)°, *V* = 1923.6(5) Å³, *Z* = 1, *ρ_{calcd}* = 1.051 Mg m⁻³, *μ* = 0.325 mm⁻¹, reflections collected: 11009, independent reflections: 6687 (*R_{int}* = 0.0267), final *R* indices [*I* > 2σ(*I*): *R*₁ = 0.0603, *wR*₂ = 0.18084, *R* indices (all data): *R*₁ = 0.0844, *wR*₂ = 0.1981; **4**: C₃₄H₁₀₆N₆Cr₂O₂Si₄, *M_r* = 1097.81, *T* = 200(2) K, monoclinic, space group *P*₂₁/*c*, *a* = 15.6863(3), *b* = 19.2132(4), *c* = 20.4594(5) Å, *β* = 93.9640(10)°, *V* = 6151.4(2) Å³, *Z* = 4, *ρ_{calcd}* = 1.175 Mg m⁻³, *μ* = 0.473 mm⁻¹, reflections collected: 52063, independent reflections: 10790 (*R_{int}* = 0.0532), final *R* indices [*I* > 2σ(*I*): *R*₁ = 0.0451, *wR*₂ = 0.1116, *R* indices (all data): *R*₁ = 0.0820, *wR*₂ = 0.1393; **5**-C₄H₁₀O: C₈₀H₁₂₂N₆Cr₂KO₈, *M_r* = 1438.94, *T* = 200(2) K, monoclinic, space group *P*₂₁/*c*, *a* = 16.4037(2), *b* = 15.7947(2), *c* = 33.2294(5) Å, *β* = 103.3030(10)°, *V* = 8378.44(19) Å³, *Z* = 4, *ρ_{calcd}* = 1.141 Mg m⁻³, *μ* = 0.362 mm⁻¹, reflections collected: 41494, independent reflections: 15013 (*R_{int}* = 0.0878), final *R* indices [*I* > 2σ(*I*): *R*₁ = 0.0720, *wR*₂ = 0.1952, *R* indices (all data): *R*₁ = 0.1300, *wR*₂ = 0.2612; **6**: C₆₆H₁₃₂N₆Cr₂KO₈Si₄, *M_r* = 1393.24, *T* = 200(2) K, tetragonal, space group *P*4₂/*c*, *a* = 16.9265(3) Å, *b* = 16.9265(3) Å, *c* = 27.3011(5) Å, *V* = 7821.9(2) Å³, *Z* = 4, *ρ_{calcd}* = 1.183 Mg m⁻³, *μ* = 0.443 mm⁻¹, reflections collected: 22457, independent reflections: 6876 (*R_{int}* = 0.0360), final *R* indices [*I* > 2σ(*I*): *R*₁ = 0.0734, *wR*₂ = 0.1985, *R* indices (all data): *R*₁ = 0.0831, *wR*₂ = 0.2088; **7**-2 C₄H₁₀O: C₇₆H₁₁₈N₆Cr₂K₂O₄, *M_r* = 1361.96, *T* = 200(2) K, monoclinic, space group *P*₂₁/*n*, *a* = 9.91160(10), *b* = 28.8440(3), *c* = 13.7416(2) Å, *β* = 90.4560(10)°, *V* = 3928.46(8) Å³, *Z* = 2, *ρ_{calcd}* = 1.151 Mg m⁻³, *μ* = 0.430 mm⁻¹, reflections collected: 36327, independent reflections: 7199 (*R_{int}* = 0.0765), final *R* indices [*I* > 2σ(*I*): *R*₁ = 0.0625, *wR*₂ = 0.1598, *R* indices (all data): *R*₁ = 0.0990, *wR*₂ = 0.1983; **8**-C₇H₈: C₈₆H₁₁₅N₆CrK₂O₆, *M_r* = 1459.04, *T* = 200(2) K, triclinic, space group *P* $\bar{1}$, *a* = 14.5434(8), *b* = 15.8602(9), *c* = 22.8046(11) Å, *α* = 78.569(3), *β* = 72.312(3), *γ* = 63.613(3)°, *V* = 4477.0(4) Å³, *Z* = 2, *ρ_{calcd}* = 1.082 Mg m⁻³, *μ* = 0.270 mm⁻¹, reflections collected: 37371, independent reflections: 15709 (*R_{int}* = 0.0530), final *R* indices [*I* > 2σ(*I*): *R*₁ = 0.0978, *wR*₂ = 0.2947, *R* indices (all data): *R*₁ = 0.1806, *wR*₂ = 0.3296; **10**: C₄₂H₅₄N₄Cr₂O₂, *M_r* = 750.89, *T* = 200(2) K, triclinic, space group *P* $\bar{1}$, *a* = 8.6139(3), *b* = 10.8806(3), *c* = 11.6811(4) Å, *α* = 83.5650(10), *β* = 81.9330(10), *γ* = 68.575(2)°, *V* = 1006.87(6) Å³, *Z* = 1, *ρ_{calcd}* = 1.238 Mg m⁻³, *μ* = 0.578 mm⁻¹, reflections collected: 13674, independent reflections: 3627 (*R_{int}* = 0.0759), final *R* indices [*I* > 2σ(*I*): *R*₁ = 0.0679, *wR*₂ = 0.1686, *R* indices (all data): *R*₁ = 0.0959, *wR*₂ = 0.1976; **11**-2 MeTHF: C₄₄H₅₆N₄Cr₂O₂, *M_r* = 776.93, *T* = 150(2) K, monoclinic, space group *P*₂₁/*n*, *a* = 10.7474(1), *b* = 22.6841(2), *c* = 17.4934(2) Å, *β* = 104.7263(6)°, *V* = 4124.71(7) Å³, *Z* = 4, *ρ_{calcd}* = 1.251 Mg m⁻³, *μ* = 0.567 mm⁻¹, reflections collected: 26280, independent reflections: 9447 (*R_{int}* = 0.0310), final *R* indices [*I* > 2σ(*I*): *R*₁ = 0.0506, *wR*₂ = 0.1484, *R* indices (all data): *R*₁ = 0.0722, *wR*₂ = 0.1654, CCDC 843643 (**3**-*n*-C₆H₁₄), 843644 (**4**), 843645 (**5**-C₄H₁₀O), 843646 (**6**), 843647 (**7**-2 C₄H₁₀O), 871483 (**8**-C₇H₈), 728851 (**10**), 728852 (**11**) contain the supplementary crystallographic data for this paper. These data can be obtained free of charge from The Cambridge Crystallographic Data Centre via www.ccdc.cam.ac.uk/data_request/cif.
- [8] R. Wolf, M. Brynda, C. Ni, G. J. Long, P. P. Power, *J. Am. Chem. Soc.* **2007**, 129, 6076.
- [9] The effective bond order is calculated based on electron occupancy of bonding and antibonding orbitals.
- [10] F. A. Cotton, L. M. Daniels, C. A. Murillo, I. Pascual, H.-C. Zhou, *J. Am. Chem. Soc.* **1999**, 121, 6856.
- [11] F. A. Cotton, C. A. Murillo, H.-C. Zhou, *Inorg. Chem.* **2000**, 39, 3728.
- [12] S. Horvath, S. I. Gorelsky, S. Gambarotta, I. Korobkov, *Angew. Chem.* **2008**, 120, 10085; *Angew. Chem. Int. Ed.* **2008**, 47, 9937.